21st Australasian Fluid Mechanics Conference
Adelaide, Australia
10-13 December 2018

An Experimental and Numerical Investigation into the Aerodynamics of the ISS Re-entry

F. Zander[1,2], D. Leiser[1], R. Choudhury[2], S. Löhle[1] and D. R. Buttsworth[2]

[1]High Enthalpy Flow Diagnostics Group, Institute of Space Systems,
University of Stuttgart, BW 70569, Germany

[2]Department of Mechanical and Electrical Engineering
University of Southern Queensland, Toowoomba, Queensland 4350, Australia

Abstract

In this work we develop a methodology for simplified calculations of the force and moment experienced by a shock impinged ISS component during atmospheric entry. Utilising blast wave theory we develop a correlation for scaling a single computationally calculated force and moment to flight relevant conditions. Our baseline computational model is selected to match a model previously tested in the TUSQ hypersonic facility. The force results of the computation match the experimental results to within 10%. With the validated computational result, we then compute the scaled loads for three different flow conditions expected to be a part of the ISS re-entry trajectory, computing an increase of axial shear force from $9.3\,kN$ to $110\,kN$ when going from an altitude of $80\,km$ down to $60\,km$. The methodology developed in this work provides a mechanism for implementing higher fidelity aerodynamic loading into break-up modelling of complex structures.

Introduction

The problem of space debris and objects entering Earth's atmosphere is becoming increasingly important as more and more vehicles and objects are being sent into space. Increasing amounts of time are spent investigating the re-entry break-up process. This includes a large amount of computational analysis, including the development of analysis codes such as ASTOS/DARS, DAS, DEBRISK, DRAMA/SESAM, DRAPS, MUSIC/FAST, ORSAT, ORSAT-J, SAM, SAPAR, and SCARAB [11, 12, 2]. Two of the fundamental limitations/restrictions of these codes are, firstly, the lack of experimental of flight data. These codes are developed based purely on theoretical evaluations and are then validated either by comparison with the very scarce measured re-entry break-up data and by each comparing the codes with each other. An additional aspect of this is that most of the codes have manually set break-up triggers, e.g. the structure will rupture at 75 km. Therefore, developing failure criteria is a critical aspect of increasing the fidelity of these analyses. Secondly, these codes have thus far only really been developed for simple, single body re-entries, such as satellites or ISS re-supply vehicles (ATV, Cygnus, etc.).

This work is investigating the next step in re-entry breakup analysis where larger, more complex vehicles will undergo atmospheric entries and break-up. This is of particular interest as it is reasonable to expect that more debris will survive the re-entry and land somewhere on Earth, presenting significant safety concerns. The largest objects that have re-entered the atmosphere thus far have been the Solyut-7 (26 m, 40 t), Skylab (26 m, 74 t) and MIR (30 m, 135 t) entries [8] which pale in comparison to the 100 m, 420 t ISS which is planned for a destructive entry within the next decade [4].

In this work we look at the effect of shock impingement which can occur in more complex structures. The satellite type, single body re-entries only have a simple bow shock forming around the front of the body which allows for comparatively simple analyses, however, in a larger more complex structure the shock resulting from the front of the body can interact with the remaining structure, causing complex, localised high heat flux and pressure regions. This is a particularly interesting aspect of the breakup as previously breakup modelling has used predominantly thermal effects for failure criteria whereas these more complex structures will require a new thinking on failure criteria, including coupled thermal and aerodynamic loading.

Using the ISS as an example case we look at the effects of these shock structure interactions, and in particular develop a methodology for the analysis. This work is a continuation of the work started in the ESA ISSABA project, presented by Zander [13], and has been continued by Leiser [9].

The main driver for this work is to provide input data for the break-up modelling community. The use of a CFD simulation for each trajectory point within a break-up simulation is computationally prohibitively expensive and hence we are developing a simplified model to provide a database of information to be fed into the break-up simulations.

Re-entry Environment

A vehicle on an atmospheric return trajectory from LEO enters the atmosphere at a speed of approximately 8 km/s. The exact trajectory is dependent on the mission history of the vehicle. We are using the ISS for this analysis, and the current plan for the re-entry is on a shallow trajectory. Given this, we have chosen to use the Cygnus OA6 shallow re-entry trajectory to define our flow conditions [10]. From the trajectory we have selected three points for detailed analysis, these are shown in table 1.

Altitude	80 km	70 km	60 km
Velocity	7668 m/s	7095 m/s	5980 m/s
Mach No.	28.0	24.4	19.1
Temperature	185.6 K	209.9 K	244.4 K
Pressure	1.0 Pa	5.5 Pa	24.0 Pa
Mass fraction, O_2	0.22	0.22	0.22
Mass fraction, N_2	0.78	0.78	0.78

Table 1: Flow conditions selected for analysis.

Re-entry Configuration

The focus of this work is on the parameterisation of the shock impingement loading on a large re-entering structure. For this study a model based on the ISS was chosen. The model chosen is representative of the Destiny, Harmony, and Columbus modules of the ISS. The experimental models are shown in figure 1. The model is analysed such that the Destiny module is the front facing part of the structure, causing a bow shock to form and impinge on the Columbus module. This particular orientation has been used for the analysis as it represents the initial re-entry configuration. We concentrate on the forces and moments

caused by the flow and shock impingement on the Columbus module.

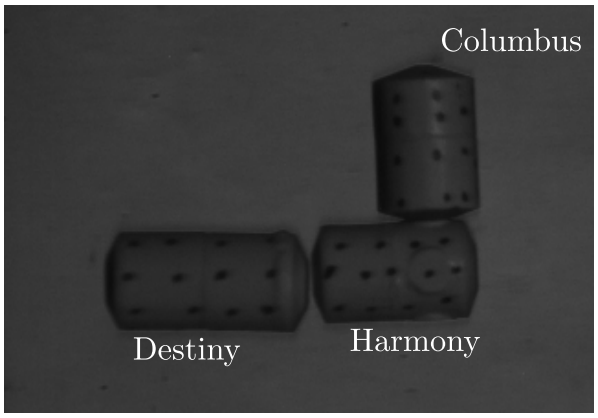

Figure 1: The experimental models of the ISS, the same geometry was used throughout the investigation.

Computational Analysis

The computational analyses in this work were done with the `Eilmer` code which was developed at The University of Queensland [5]. This multi-block, Navier-Stokes solver, which was developed for hypersonic application, has been well validated in this flow regime. For the reacting gas cases, not shown here but used for the blast wave theory validation, the 5-species variation of the Gupta air chemistry model was used [6].

The outcomes of the earlier parts of this study showed that a significant issue with the analysis of this problem is the amount of computational time required [13]. A full computational analysis is prohibitively expense driving the need to develop a technique for simplifying the overall analysis.

A full analysis requires the CFD analysis of the full trajectory, including a full chemical reaction scheme. The reacting flow analysis is critical as the reactions absorb a significant amount of flow energy which then does not get absorbed by the structure. The other component of this is that the shock shape, and hence the impingement locations are also modified by the real gas effects.

Our main focus in this work is the bow shock impingement, and the resulting forces and moments on a lateral structure, herein described as a 'vertical arm'. An ideal gas analysis will give a reasonable indication of the pressure forces experienced, the error will be less than ∼15%[7], and give a good estimate of the loading. The three-dimensional pressure distribution of the ideal gas should be fairly similar in form to the reacting gas case, however, the locations will be incorrect due to the shock form being incorrect. To account for this, we propose using the pressure distribution from an ideal analysis, and then scaling the distribution to the real gas locations.

Blast Wave Theory

For the distribution scaling we utilise the approach suggested by Fritsche [3] and use blast wave theory [1] to estimate our shock impingement location. We then scale our force distribution calculated using ideal gas CFD and then calculate the overall force and moment on the arm.

Blast wave theory has long been used for the estimation of shock locations around simple bodies [1]. This analysis allows the computation of the shock radius around a body dependent on the axial location, Mach number and body diameter. The

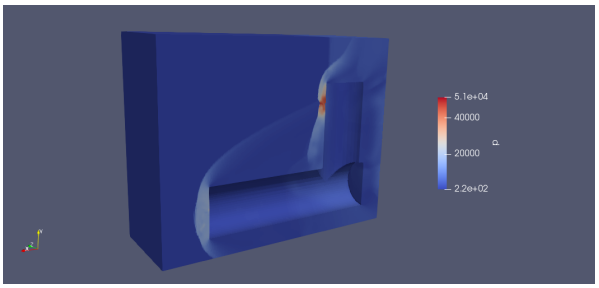

Figure 2: A sample computational result showing the computational domain.

formulation we use is the so-called *second approximation of the blunt-nosed cylinder*, shown in equation (1). It should be noted that the blast wave theory is only applicable away from the nose region.

$$\frac{R/d}{M_\infty C_D^{0.5}} = 0.795\sqrt{\frac{x/d}{M_\infty^2 C_D^{0.5}}\left[1+3.15\frac{x/d}{M_\infty^2 C_D^{0.5}}\right]} \qquad (1)$$

where R is the shock radius, d the body diameter, M_∞ the free-stream Mach number and C_D the coefficient of drag. This calculation is known to have a downstream offset in the result and here we have elected to use a body diameter length (2.7 m) to correct for this. A sample result of this is compared to the 2D axisymmetric CFD to verify the methodology. Figure 3 shows the comparison and a very good agreement is evident.

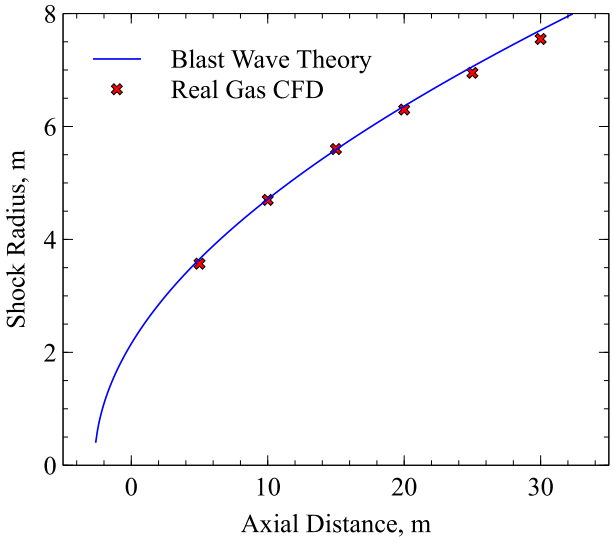

Figure 3: A comparison of the shock radius using the blast wave theory with the reacting CFD at the 70 km altitude flow condition.

Scaling

In this work we are assuming that the drag coefficient of the model can be used for scaling. However, this assumption is limited to the case where the shock impingement occurs at the same relative location up the arm, i.e. if the shock hits the arm at the half way mark in the small scale model, then it must also hit halfway up on the large scale model. The shock impingement location is dependent on two parameters, the Mach number and the axial location to model diameter ratio.

Using the blast wave theory allows us to compute the limits at

which the Mach number no longer changes the shock impingement location, i.e. the hypersonic limit for this geometry. This is done by computing the radial location of the shock in limiting case as Mach number approaches infinity (we used $M = 100$), and then calculating the lowest Mach number which results in approximately the same radial location (we used a 10% accuracy for this first analysis). The result of this is shown in figure 4 as the blue line. The region under the limit is where the drag coefficient is dependent on both the Mach number and the x/D and above the limit there is no longer the Mach number dependency.

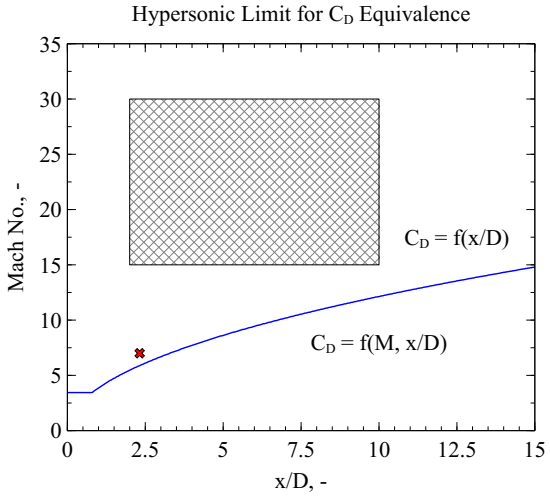

Figure 4: The hypersonic limit of the drag coefficient scaling. Above the limit (blue line) the Mach number no longer has an effect on the drag coefficient. The square region shows the parameter region of particular interest for re-entry modelling. Our experimental point is marked with the red square.

With the determination of of Mach number independence of the drag coefficient, we can then compute the force experienced by the vertical arm based on a scaled model using the formulation shown in equations 2 – 4. It must be remembered that this scaling only works if the x/D is matched.

$$F = \frac{C_D \cdot \rho \cdot A \cdot v^2}{2} \tag{2}$$

$$C_D = \frac{2 \cdot F_{model}}{A_{model} \cdot \rho_{model} \cdot v^2_{model}} = \frac{2 \cdot F_{flight}}{A_{flight} \cdot \rho_{flight} \cdot v^2_{flight}} \tag{3}$$

$$F_{flight} = F_{model} \cdot \frac{A_{flight}}{A_{model}} \cdot \frac{\rho_{flight}}{\rho_{model}} \cdot \frac{v^2_{flight}}{v^2_{model}} \tag{4}$$

The analysis of F_{model} is done cell-by-cell in the computational model. At each cell the F_x, F_y and F_z are calculated based on the pressure in the cell, the wall area and the surface normal.

The cell-by-cell treatment accounts for the flow field variations, in particular those caused by the shock impingement. The spatially resolved forces are also used for the moment calculation, for the scaled calculation the F_{flight} force is used with the scaled y (vertical) distance as shown in equation 5.

$$M_{z,flight} = F_{flight} \cdot y_{flight} \tag{5}$$

This analysis allows us to limit the number of computations required for determining the force and moment on the vertical arm. Every point above the hypersonic limit can be determined through a simple flow and geometric scaling of a loading computed at the same x/D. As is shown in figure 4 the primary conditions of interest for break-up analyses lie above the hypersonic limit. This allows the easy build up of a force and moment database with minimal computational requirements by computing the loading at discrete x/D locations along the limit line and then using the scaling, and interpolation if necessary, to calculate the loading for a specific flight condition.

Results

Experimental

Validation of the ideal gas CFD was undertaken using the TUSQ Luwieg Tube facility at the University of Southern Queensland. The TUSQ facility produces cold, i.e. ideal gas, hypersonic flows which can be used for aerodynamic measurements. In this campaign 400:1, ρL scaled models of the ISS subsection were tested.

A comparison of the CFD and experimental results is shown in figure 5, this shows the Schlieren result of the experiment overlaid with the pressure contours of the CFD.

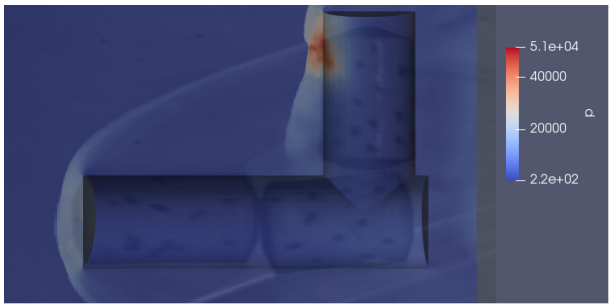

Figure 5: A comparison of the experimental Schlieren and computational results.

The numerical results of the small scale model resulted in a force of $F_x = 1.0N$ and a moment of $M_z = 0.011N \cdot m$.

The calculated x-force compares very well with the experimental results, $F_x = 1.1N$, measured by Leiser [9]. These force results show that the simulation models the tunnel flow, and the force of the fluid structure interaction very well.

Flight Loading

In this work we are using our 1:400 scale model of the ISS components as a reference. Therefore, the scaling of the CFD computed the force is scaled by 400×400 (for both spatial dimensions), the ratio of the densities, $\rho_{flight}/\rho_{model}$, and the ratio of the velocities squared, v^2_{flight}/v^2_{model}. The moment calculation is additionally scaled by 400 to account for the moment arm in one spatial direction (in addition to the force modification).

The CFD of the TUSQ size model calculated an F_x force of $1.0N$, and a M_z of $0.011Nm$. The results of scaling the calculated forces to the ISS flight size and flow conditions are presented in table 2.

The three sets of force and moment data were calculated based off the same CFD result using the scaling theory presented in equations 4 & 5. The ability to rapidly calculate the loads on the structure based off a single CFD result, for a given x/D, opens up the possibility of more complex load analyses within

	F_x	M_z
80 km	9.31 kN	40.39 kN·m
70 km	41.45 kN	179.82 kN·m
60 km	109.85 kN	476.57 kN·m

Table 2: Forces and moments calculated using the scaling theory on the computational result.

a break-up modelling analysis.

Future Work

The next step is this work is to build-up a database of forces and moments. This will give a database of loads and moments which can be implemented into break-up models to enable more realistic failure mechanisms to be incorporated.

Within this body of work we have concentrated on the pressure and moment loads experienced by vehicle during the atmospheric entry, with particular emphasis on the effects of the shock impingement. In the next step this needs to be coupled with the thermal loading of the re-entry so that the failure criteria in the breakup modelling can utilise the coupled thermo-mechanical loading.

Conclusions

In this work we have developed a new methodology for calculating the force and moment experienced by a shock impinged arm during an atmospheric entry. Utilising blast wave theory to calculate the shock shape as a function of Mach number and x/D of our model allows us to define a hypersonic limit above which we can undertake drag coefficient scaling. The drag coefficient scaling allows the force and moments calculated using CFD to be scaled for different flow conditions.

We computed the force and moments for a single geometry and flow condition using a 3D CFD simulation and verified these results experimentally obtaining an axial force of $F_x = 1.0N$ compared to the experimental result of $F_x = 1.1N$. The CFD result was then used as the basis for computing the force and moment at three different trajectory points of the anticipated ISS re-entry.

This work has provided a methodology for producing a database of loads which can be implemented in re-entry break-up modelling simulations.

Acknowledgements

This work has been supported by the ESA project 'ISS Atmospheric Break-up Analysis' (Contract No.4000116300), the DAAD exchange program (Project ID 57319260) and the DLR Project "VerKritRS" (Contract No. 50LZ1704).

References

[1] Anderson, J.-D., *Hypersonic and High-Temperature Gas Dynamics*, McGraw-Hill, 2006.

[2] Annaloro, J., Galera, S., Kärräng, P., Prigent, G., Lips, T. and Omaly, P., Comparison between two spacecraft-oriented tools: Pampero & SCARAB *Journal of Space Safety Engineering*, **4**, 2017, 15–21, doi:10.1016/j.jsse.2017.02.004.

[3] Fritsche, B., Kärräng, P. and Lips, T., ISS SCARAB Modelling, *Tech Report*, ISSABA-FP, ESA, 2017.

[4] Gray, C., ISS end of life strategy and contingency action plan, *Technical Report*, SSP 51066, NASA, 2016.

[5] Gollan, R.-J. and Jacobs, P.-A., About the formulation, verification and validation of the hypersonic flow solver eilmer, *International Journal for Numerical Methods in Fluids*, **73**, 2013, 19–57, doi:10.1002/fld.3790.

[6] Gupta, R.-N., Lee, K.-P., Thomson, R.-A. and Yos, J.-M., A review of reaction rates and transport properties for an 11-species air model for chemical and thermal nonequilibrium calculations to 30000K, *Technical Report*, TM 85820, NASA, 1990.

[7] Huber, P.-W., Hypersonic Shock-Heated Flow Parameters for Velocities to 46,000 feet per second and altitudes to 323,000 feet, Technical Report, NASA TR R-163, 1963.

[8] Klinkrad, H., *Space Debris Models and Risk Analysis*, Springer, 2006.

[9] Leiser, D., Zander, F., Löhle, S., Buttsworth, D.-R. and Choudhury, R., Aerodynamic separation of re-entering spacecraft: experiments and numerical rebuilding, *4th International Space Debris Re-entry Workshop*, Darmstadt, Germany, 2018.

[10] Löhle, S., Jenniskens, P., Lips, T., Bastida-Virgili, B., Albers, J., Zander, F., Krag, H., Grinstead, J.-H. and Bacon, J., Preparations of the airborne ATV-5 re-entry observation campaign, *12th International Planetary Probe Workshop*, Cologne, Germany, 2015.

[11] Lips, T. and Fritsche, B., A comparison of commonly used re-entry analysis tools, *Acta Astronautica*, **57**, 2005, 2–8, doi:10.1016/j.actaastro.200503.010.

[12] Préveraud, Y., Vérant, J.-L., Balat-Pichelin, M. and Moschetta, J.M., Numerical and experimental study of the thermal degradation process during the atmospheric re-entry of a TiAl6V4 tank, *Acta Astronautica*, **122**, 2016, 258–286.

[13] Zander, F., Löhle, S., Krag, H., Lemmens, S., Gollan, R.-J. and Jacobs, P.-A., Numerical Flow Analysis of the ISS Re-Entry, *Proc. 7th European Conference on Space Debris*, Darmstadt, Germany, 2017.